ELSEVIER

Powder Technology 98 (1998) 38–47

POWDER TECHNOLOGY

Computer simulation of bubbles in large-particle fluidized beds

D. Gera [a,b,*], M. Gautam [a], Y. Tsuji [b], T. Kawaguchi [b], T. Tanaka [b]

[a] *Department of Mechanical and Aerospace Engineering, West Virginia University, Morgantown, WV 26506-6106, USA*

[b] *Department of Mechanical Engineering, Osaka University, Yamada-oka, 2-1, Suita, Osaka 565, Japan*

Received 27 October 1997; received in revised form 20 January 1998

Abstract

A distinct element model is used to study the hydrodynamics of large-particle fluidized beds. The computed bubble rise velocity, voidage variations, averaged particle/particulate and fluid velocities are compared with the other continuum theory based on two fluid model. Based on the averaged particle/particulate velocities in a grid cell, deformation of the particle layers predicted by the two fluid model and the distinct element method are also compared. The predicted characteristics of bubble formation, motion, and eruption at the bed surface are in good qualitative agreement with the experimental observations. The quantitative differences in predicting the above parameters along with the advantages and limitations of two approaches for the case of a single isolated bubble rising in a two-dimensional fluidized bed are discussed.
© 1998 Elsevier Science S.A. All rights reserved.

Keywords: Fluidized bed; Bubbles; Two fluid model; Distinct element model

1. Introduction

In the early 1960s, using the solutions of the potential flow theory for a flow over a sphere and Darcy's law for relating the pressure gradient with the relative velocities of the two phases, Davidson [1] gave the first theoretical treatment to the problem of a single isolated bubble rising in an unbounded fluidized bed. Davidson assumed the circular shaped bubble to be free of any solid particles, and treated the voidage of the particulate phase to be constant and equal to the voidage at the minimum fluidization (ϵ_{mf}) inside the bed. Relaxing the assumption of constant voidage, Jackson [2] treated the voidage to be a dependent variable, and developed a more detailed set of mathematical equations to investigate the hydrodynamics and stability of bubbles in fluidized beds. In a sequel, Anderson and Jackson [3], using the spatial averaging techniques for translating the point Navier–Stokes equations for fluid and Newtonian equations of motion for particles, derived the fluid-particle and particle–particle interaction terms in the momentum balance equations. Following the work of Anderson and Jackson [3], many researchers solved these complete set of mass and momentum balance equations to obtain fluid and particulate flow field solutions.

Nowadays, while modeling fluidized beds, two theories, (i) one based on molecular dynamics, and the other (ii) based on the assumption that the gas and particulate phases form two inter-penetrating continua, have been used in the literature. Based on the molecular dynamics, two approaches, viz. soft sphere approach and a hard sphere approach are used in the discrete particle simulations of the fluidized beds. In the soft sphere approach, it is possible to estimate the interaction forces using multiple particle contacts which are of prime importance in modeling the quasi-stationary systems [4,5]. Hard sphere approach is a quasi-instantaneous and the particle interaction is based on binary collisions. A characteristic feature of hard sphere simulations is that the sequence of collisions is processed one at a time, and the collision partners and sequences are chosen based on the relative approach velocities of the particles [6]. In general, discrete models are powerful investigative tools which allow the direct feasibility studies of the effect of individual particles' physical properties such as its size, shape, and density on the resulting motion of a fluid in a fluidized bed. The other theory, based on the interpenetrating fluids, commonly referred to as 'Two Fluid Model' (TFM) approach, considers all the solid particles to be identical, characterized by their mean diameter and density. Syamlal et al. [7] extended this technique to develop multi particle systems which can be used to describe the fluidization of several different types of particles, treating

* Corresponding author. Tel.: (801) 378-9178; Fax: (801) 378-5037; E-mail: gera@et.byu.edu

0032-5910/98/$19.00 © 1998 Elsevier Science S.A. All rights reserved.
PII S0032-5910(98)00017-5

each one of them as a separate phase. Often, the velocity and the stress distributions within the flowing bulk in TFM are assumed to be of certain uniform and continuous functional form which are incorporated in the momentum balance equations using empirical correlations. However, in the discrete models, these assumptions need not be made since the motion of each single particle is directly calculated by accounting for the interactions with the other particles and the fluid phase. A discrete particle simulation approach provides a unique insight into bed hydrodynamics. Particles with different geometrical shapes, approximated by polygons with 72 sides, have been tried using the present method [T. Kawaguchi, Osaka University, Private Communication, 1995.], and it is far more difficult, if not impossible, to account for this condition in TFM.

Discrete models are conceptually simpler but rely heavily on the computing power when simulating medium-to-large scale systems. The distinct element method (DEM), based on the soft sphere approach of molecular dynamics, involves the application of Newtonian dynamical equations to a system of colliding particles. Cundall and Strack's [8] distinct element model is the best known formalized model which uses the solution of Newtonian dynamical equations to compute the contact forces. On the other hand, continuum models assume the particulate or granular media to behave as a fluid. These approaches are mathematically complicated, but rely strongly on the empirical correlations for few key parameters, such as the solid's viscosity, and solid's pressure among others. Gabor [9] found that a Bingham plastic model for the particulate phase provided a better approximation for the rheology of fluidized powders as compared to Newtonian or power-law models. The kinetic theory of granular flow also allows the computation of the rheology of the mixture with the empirical input of normal and tangential restitution coefficients. Gidaspow [10] elaborates the dramatic effect of the normal restitution coefficient on the computed viscosity. Lun et al. [11] have shown that the solid pressure for the granular media can be computed through the input of restitution coefficient and the coefficient of friction between the different particulate phases. However, many researchers still compute the solid's pressure by performing a curve fit on Musters and Rietema's [12] experimental data of bed deformation.

Cranfield and Geldart [13] calculated the visible bubble flow from experimental data in two-dimensional beds of large particles (1–2 mm diameter), and found that only 55% of the excess gas flow passed through the bed as visible flow and the remaining 45% passed through the bubbles and also percolated through the particulate phase. More recently, Yates et al. [14] attributed the high voidage near the bubble to increased interstitial flow and increased throughflow. It is important to predict the throughflow component accurately because the pattern of gas flow through the bubbles has an effect on the degree of gas–solids contacting. The throughflow velocity (U_{th}) of the gas, also known as 'invisible flow' is defined as the component of fluid flow in a bubble, relative to the bubble, across a plane normal to the vertical axis of the bubble. Also, an accurate prediction of the rate of interphase mass transfer, a function of throughflow velocity, is needed for the design of efficient chemical reactors.

Fluidized bed reactors are ideal for gasifying coal due to higher rates of heat and mass transfer and solid's mobility. However, scale-up is one of the largest concerns for using the fluidized beds to commercialized gasification of coal. This is due to the absence of an experimentally verified hydrodynamic theory that can describe the complicated transient gas and solid motion in a fluidized bed [15]. It is convenient to carry out detailed fluid dynamic investigations on small beds at ambient conditions. However, similitude (dimensional analyses) techniques need to be developed further so as to assure the confidence in duplicating the experimental results of large reactors from the small scale laboratory simulations. A recent survey by Glicksman et al. [16] identifies the key parameters for continuum models which must be included in scaling so as to preserve the dynamic similarities between the large scale commercialized beds and small scale model simulations. A limiting factor in discrete particle models is the number of particles which can be handled in a simulation. With the advent of vector and parallel machines, it is still not possible to use the discrete particle simulation for a complete fluidized bed of industrial scale.

2. Theoretical formulations

2.1. Distinct element method

In a fluidized bed, the particle motion is induced by the fluid drag force and the trajectories of individual particles are affected by the presence of other particles and gravity. Therefore, the instantaneous velocities and position of the particles are to be calculated by taking into account the sum of the fluid drag force ($\vec{f}_D$), the inter particle contact force ($\vec{f}_C$), and the gravity force ($m\vec{g}$). Using Newton's second law of motion, the translational motion of a single particle in terms of these forces can be expressed as:

$$\dot{\vec{v}}_s=(\vec{f}_C+\vec{f}_D)/m+\vec{g} \tag{1}$$

where $\vec{v}_s$ is the particle velocity, m is the mass of the particle, $\vec{g}$ is the acceleration due to gravity, and the quantity $(\cdot)$ represents the time derivative.

In such simulations where all the particles are suspended in the fluidizing stream, if the time step in the numerical integration is chosen to be sufficiently small, then it can be safely assumed that the single time step disturbances are confined to its immediate neighbors only. Therefore, in calculating the instantaneous motion of particles, only the contact forces resulting from the particle and its immediate neighbors are considered, and the disturbances from the remote particles are neglected. Furthermore, the contact forces consist of normal ($\vec{f}_{Cn}$) and tangential ($\vec{f}_{Ct}$) forces, which are modeled using Cundall and Strack's [8] mechan-

ical model of a spring, dashpot, and a friction slider as shown in Fig. 1. In this model, the normal and tangential component of forces are expressed as the sum of forces due to the springs and dash pots, and the normal and tangential velocities are expressed in terms of the slip velocity (or relative velocity, $\vec{v}_r$) of the contact point in the following manner:

$$\vec{f}_{Cn}=-k\vec{d}_n-\eta\vec{v}_n \tag{2}$$

$$\vec{f}_{Ct}=-k\vec{d}_t-\eta\vec{v}_t \tag{3}$$

$$\vec{v}_t=\vec{v}_r-\vec{v}_n \tag{4}$$

$$\vec{v}_n=(\vec{v}_r.\vec{n})\vec{n} \tag{5}$$

where $\vec{d}_n$ and $\vec{d}_t$ are the particle displacements in the normal and tangential directions, respectively, k is the stiffness of the spring, η is the viscous dissipation coefficient.

If there is a sliding between the particles, which is checked by the Coulomb-type friction law, i.e.

$$|\vec{f}_{Ct}|>\mu_f|\vec{f}_{Cn}| \tag{6}$$

where μ_f is the friction coefficient, then the tangential force is modeled by the following equation instead of Eq. (3).

$$\vec{f}_{Ct}=-\mu_f|\vec{f}_{Cn}|\vec{t} \tag{7}$$

where $\vec{t}$ is a unit vector defined by $\vec{t}=\vec{v}_t/|\vec{v}_t|$. Spring stiffness ($k$), η and μ_f are the input parameters to DEM. Stiffness (k) is calculated from the Hertzian contact theory in terms of the material's physical properties, such as Young's modulus and Poisson ratio [4]. Artificially reducing the spring stiffness up to a certain critical value, k_{cr} would not have any significant effect on the individual particle motion. If a very soft spring is used for the computations then the particles would practically embed into each other by causing a greater overlapping region. In such a case, with very small stiffness, voidages in some grid cells could go to an impossibly low value of zero. However, in the modeling of the systems where particles fall under gravity in the absence of fluidization stream, for example in a hopper or a chute, the spring stiffness needs to be determined very accurately. Because, in such a case, the effects of disturbances from the remote particles would have a stronger influence in the calculation of the contact forces.

The damping coefficient (η) is determined by expressing the solution of equation of motion for the mass, spring, and a dashpot oscillating system in terms of the ratio of the final velocity of the mass to its initial velocity (i.e., coefficient of restitution, e) as

$$\eta=2\sqrt{mk}\frac{\ln(1/e)}{\sqrt{\pi^2+(\ln(1/e))^2}} \tag{8}$$

In a mechanical model of spring, dashpot, and a friction slider, two particles move towards each other until the contact force changes its sign, i.e., from attraction to repulsion. In such a model, two characteristic times exist, i.e., (i) when the relative displacement between the particles becomes zero, and (ii) when the contact force acting on the particles becomes zero. In the present case, the coefficient of restitution is defined by taking the ratio of the final velocity at the time when the relative displacement become zero to the initial velocity of the particle. For the hypothetical case of a very small coefficient of restitution (say around 0.1), a non linear spring (where the force varies to some power of the displacement, e.g., $F=-kx^n$, where n is a positive integer greater than 1) would yield better results for the damping coefficients than the linear spring model ($F=-kx$). In the simulation of fluidizing beds, the net contact force on each particle is calculated by the summation of all the contact forces originated from its immediate neighbors. The interaction of a particle with the wall is modeled in a same manner as a particle-to-particle contact, except that the wall is stationary.

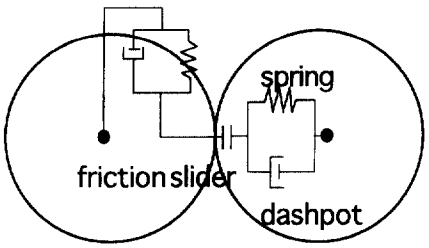

Fig. 1. Contact force model.

The rotational motion is assumed to be caused by inter-particle contact forces only, and may be expressed as:

$$\dot{\vec{\omega}}=\vec{T}/I \tag{9}$$

where $\dot{\vec{\omega}}$ is an angular acceleration, T is the net torque caused by the contact forces, and I is the mass moment of inertia of the particle.

After modeling the contact forces, the new velocities and the position after the time step (Δt) are calculated by integrating Eqs. (1)–(9):

$$\vec{v}_s=\vec{v}_{s0}+\dot{\vec{v}}_{s0}\Delta t$$

$$\vec{r}=\vec{r}_0+\vec{v}_s\Delta t$$

$$\vec{\omega}=\vec{\omega}_0+\dot{\vec{v}}\,\omega_0\Delta t \tag{10}$$

where subscript 0 denotes the values at the previous time step, and $\vec{v}_s$, $\vec{r}$, and $\vec{\omega}$ represent the particle's velocity, position, and the angular velocity, respectively at the new time step. Some of the mathematical manipulations in the formulation of equations are omitted here and can be directly viewed from Ref. [4].

In the present approach, the determination of the critical time step ($t_{cr}=2\pi(m/k)^{1/2}$) for numerical integration is based on a single-degree-of-freedom system of mass m, connected to the ground by a spring of stiffness k. In this approach, to avoid numerical instabilities and to decrease the CPU time, a larger 'integration time-step' is deduced by con-

sidering the interaction between the particles to be softer than the actual values obtained from the elastic moduli of the particles. From our trial calculations, it is seen that artificially reducing the stiffness up to some critical value (when the overlapping of the particles becomes less than 1/100th of the particle diameter) would not cause any significant difference on the individual particle motion. It should be mentioned here that for models with instantaneous impacts (hard sphere approach), the minimum time step required is usually based on the minimum time between inter-particle collisions. This minimum value is related to the maximum relative velocities between particles during a simulation.

2.1.1. Fluid motion

Following the analyses of Anderson and Jackson [3], the continuity and momentum equations for the fluid phase can be written in terms of locally averaged variables as

$$\frac{\partial}{\partial t}(\epsilon\rho_g)+\nabla.(\epsilon\rho_g v_g)=0 \tag{11}$$

$$\frac{\partial}{\partial t}(\epsilon\rho_g v_g)+\nabla.(\epsilon\rho_g v_g v_g)=-\epsilon\nabla P+\beta(v_s-v_g)+\epsilon\rho_g g \tag{12}$$

where ϵ is the voidage fraction, ρ_g, v_g, and P are the density, velocity, and pressure of the gas, respectively, and β is the fluid particle interaction coefficient, which is given by,

$$\beta=\begin{cases}150\dfrac{(1-\epsilon)^2}{\epsilon d_p^2}\mu_g+1.75(1-\epsilon)\dfrac{\rho_g}{d_p}|v_s-v_g| & \epsilon\le 0.8\\ \dfrac{3}{4}C_D\dfrac{\epsilon(1-\epsilon)}{d_p}\rho_g|v_s-v_g|\epsilon^{-2.7} & \epsilon>0.8\end{cases} \tag{13}$$

The drag coefficient for an isolated particle depends on the particle Reynolds number (Re), and is given by:

$$C_D=\begin{cases}24(1+0.15\mathrm{Re}^{0.687})/\mathrm{Re}, & \mathrm{Re}<1000\\ 0.43, & \mathrm{Re}\ge 1000\end{cases} \tag{14}$$

A fixed bed configuration is used as an initial condition for the particles in the present study which was simulated by randomly placing 22 000 particles, separated by a minimum distance of at least one particle diameter, in a rectangular domain of 0.6×1.0 m and allowing them to fall freely under the gravity in vacuum until they are completely settled in the bed (Fig. 2). The set of constitutive equations supplemented with the initial and boundary constraints are solved explicitly for particles motion and the set of conservation equations along with the boundary conditions are solved iteratively using the semi-implicit method for the pressure linked equations (SIMPLE) for fluid motion.

2.2. Two fluid model

In simulating a two-dimensional fluidized bed using two fluid model, the complete set of conservation equations of

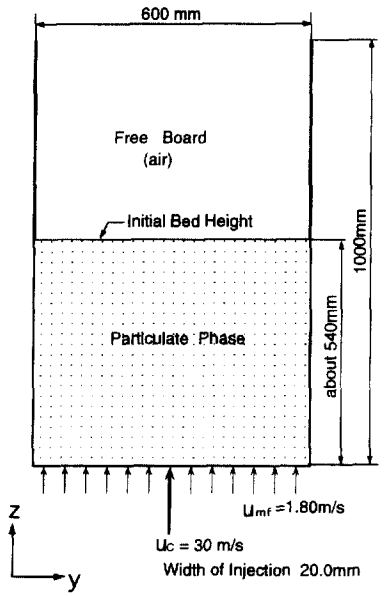

Fig. 2. Fluidized bed configuration.

mass and momentum, for a gas phase and interpenetrating granular/particulate phase are given by [17,18]:

Continuity equations:

$$\frac{\partial}{\partial t}(\epsilon\rho_g)+\nabla.(\epsilon\rho_g v_g)=0 \tag{15}$$

$$\frac{\partial}{\partial t}[(1-\epsilon)\rho_s]+\nabla.[(1-\epsilon)\rho_s v_s]=0 \tag{16}$$

Momentum balance equations:

$$\frac{\partial}{\partial t}(\epsilon\rho_g v_g)+\nabla.(\epsilon\rho_g v_g v_g)=-\epsilon\nabla P+\beta(v_s-v_g)+\epsilon\rho_g g \tag{17}$$

$$\frac{\partial}{\partial t}[(1-\epsilon)\rho_s v_s]+\nabla.[(1-\epsilon)\rho_s v_s v_s]=-(1-\epsilon)\nabla P +\nabla.S_s+\beta(v_g-v_s)+(1-\epsilon)\rho_s g \tag{18}$$

and

$$S_s=\begin{cases}-P_s^p I+\mu_s^p[\nabla v_s+\nabla v_s^T] & \text{if } \epsilon\le\epsilon^*\\ -P_s^v I+\mu_s^v[\nabla v_s+\nabla v_s^T]+0.5\lambda_s^v tr[\nabla v_s+\nabla v_s^T] & \text{if } \epsilon>\epsilon^*\end{cases} \tag{19}$$

where ϵ is the voidage fraction, ρ_g, ρ_s, v_g, and v_s are gas density, solid's density, gas velocity, and the solid's velocity, respectively; P and P_s are the gas pressure and the solid's pressure, respectively; β is the gas–solid interaction coefficient given by Eq. (13), g is the acceleration due to gravity, and I and S_s are unit tensor and the solid's stress tensor, respectively. The significance and modeling of the solid's pressure and rheology are discussed in Section 2.2.1.

2.2.1. Solid's pressure and viscosity

Solid's pressure, P_s, appearing in Eq. (19) represents the reaction force that imposes the incompressibility constraint

which is similar to the pressure in the incompressible fluid. In the equations governing the flow of fluidized systems, P_s is normally treated as a dependent variable and a function of voidage of the following form:

$$\nabla P_s = G(\epsilon)\nabla\epsilon; \tag{20}$$

where $G(\epsilon)$, referred to as the modulus of elasticity, represents the particle-to-particle interaction coefficient. In the present simulations, if the computed voidage is about to go lower than the value of ϵ^* (normally referred to as compaction gas phase volume fraction), then the void fraction is held constant at this minimum value and solids pressure, P_s is computed as a dependent variable of the voidage. In fact, modeling the particle's pressure and solid's rheology has always presented a problem. In extreme cases, some researchers have ignored them all together because of the lack of experimental data, others have taken solids pressure equal to the fluid pressure and solid's viscosity to be a some constant which was assigned a greater value than the fluids shear viscosity. Solid's pressure, if treated as an independent variable, will cause closure problems, i.e., the number of unknowns will exceed the number of equations. In the literature, mostly it is assumed to be of some empirical function of the voidage. Based on the experimental results of Musters and Rietema [12], many researchers while modeling the fluidized beds using two fluid theory used a wide range of empirical correlations for $G(\epsilon)$, ranging from the exponential functions of the form [$G(\epsilon)=Ae^{B(\epsilon^*-\epsilon)}$, where A and B represent the normalizing units factor and compaction modulus, respectively] to algebraic power form [$G(\epsilon)=A(\epsilon^*-\epsilon)^B$]. Massoudi et al. [19] present a brief overview of these different correlations cited in the literature and their impact on the simulation of fluidized beds. This term, $G(\epsilon)$, becomes really significant when the void fractions go below a certain minimum value, ϵ^*. This parameter is used to avoid numerical instabilities, and to prevent void fraction from reaching impossibly low values. In physical terms, the value of the elasticity coefficient (G) depends on the bed porosity, i.e., when the bed expands, the powder structure becomes looser and weaker, so that the (G) will be reduced. The particular choice of ϵ^* would result in a rapidly decreasing solid phase modulus for if ϵ is greater than ϵ^*, and a rapidly increasing solid phase modulus if ϵ is less than ϵ^*, thus preventing the solids phase volume fraction to becoming much larger than $(1-\epsilon^*)$ [20]. It should be pointed out that in case of the beds with more than one particulate phase, the coefficient of friction may be used to calculate the momentum transfer between the particulate phases. Gidaspow [21,10] also gives a brief review of this assumption, and many other constraints required for modeling solids pressure and viscosity using kinetic theory approach. In the kinetic theory approach, solids pressure (P_s) and the viscosity (μ_s) are defined by the two separate functions in the frictional (when $\epsilon \le \epsilon^*$) and non-frictional (when $\epsilon > \epsilon^*$) regimes in the following way.

For frictional regime (when $\epsilon \le \epsilon^*$):

$$P_s^f = (1-\epsilon)P^* \tag{21}$$

$$\mu_s^f = \frac{P^*\sin\phi}{2\sqrt{I_{2D}}}$$

$$P^* = 10^{24}(\epsilon-\epsilon^*)^{10} \qquad \epsilon<\epsilon^* \tag{22}$$

where I_{2D} is the second invariant of the strain rate tensor, and ϕ is the angle of internal friction. For non-frictional regime (when $\epsilon > \epsilon^*$)

$$P_s^c = 2(1+e)\rho_s g_0 \epsilon_s^2 \Theta \tag{23}$$

$$\mu_s^c = K_2 \epsilon_s \sqrt{\Theta} \tag{24}$$

$$\lambda_s^c = K_1 \epsilon_s \sqrt{\Theta}$$

$$K_1 = \frac{4 d_p \rho_s (1+e)\epsilon_s g_0}{3\sqrt{\pi}} - \frac{2}{3}K_2$$

$$K_2 = \frac{d_p \rho_s}{2}\left[\frac{\sqrt{\pi}}{3(3-e)}(1+0.4(1+e)(3e-1)\epsilon_s g_0) + \frac{8\epsilon_s g_0(1+e)}{5\sqrt{\pi}}\right] \tag{25}$$

$$g_0 = \frac{1}{\epsilon}\left(1+\frac{3}{2}\frac{\epsilon_s}{\epsilon}\right) \tag{26}$$

In the present computations, we tried three cases, viz. (i) taking solid's (particulate phase) viscosity as a constant in the bed, (ii) solid's viscosity to be zero, and (iii) solid's viscosity modeled through Eqs. (21) and (24).

The conservation equations are solved on a staggered grid using Multiphase Flow with Interphase eXchanges (MFIX) computer code developed by Morgantown Energy Technology Center [7]. The convective terms in the conservation equations are discretized using a second-order flux limiter method which is essentially a sum of an UPWIND flux plus a correction term of the order of $0.5|U|\epsilon_i - \epsilon_{i-1})\phi_i$ (where U is the velocity and ϵ_i is the voidage at ith cell, ϕ_i is the superbee flux limiter [22]. Recently, Gera et al. [23] showed the tremendous influence of the numerical inaccuracies in the first order UPWIND techniques, which leads to a strong artificial numerical diffusion in the solution of governing equations which is orders of magnitude greater than the naturally appearing diffusion terms in the equations. In the present simulations, the mass balance equations are fully differenced implicitly, and convective and diffusive terms in the momentum equations are discretized explicitly.

2.3. Simulation conditions and input parameters

The simulation conditions and the input parameters for TFM and DEM approaches are listed in Table 1. In the present case, the bed width is deliberately chosen to be 0.6 m so as to give a good contrast in the prediction of bubble character-

Table 1
Simulation conditions for DEM and TFM

Discrete Element Method (DEM)	Two Fluid Model (TFM)
Particle shape: spherical	Particle shape: spherical
Diameter: 0.004 m	Diameter: 0.004 m
Density: 2700 kg/m^3	Density: 2700 kg/m^3
Stiffness: 800 N/m	$\epsilon_{initial} = 0.431$; $\epsilon^* = 0.43$
Coefficient of restitution, $e = 0.9$	Coefficient of restitution, $e = 0.9$
Coefficient of friction: $\mu = 0.3$	Angle of repose $\phi = 40^\circ$
Number of particles: 22 000	Gas density = 1.205 kg/m^3
Gas density = 1.205 kg/m^3	Gas viscosity = 1.8×10^{-5} kg/m s
Gas viscosity = 1.8×10^{-5} kg/ms	Cell size: 0.02×0.02 m
Cell size 0.02×0.02 m	Bed width × height: 0.6×1 m
Bed width × height: 0.6×1 m	Packed bed height: 0.54 m
Approx. packed bed height: 0.54 m	Jet width: 0.02 m: Jet location: center
Jet width: 0.02 m; Jet location: center	Jet velocity: 30 m/s for 0.4 s
Jet velocity: 30 m/s for 0.4 s	Minimum fluidization velocity: 1.8 m/s
Minimum fluidization velocity: 1.8 m/s	(to all the bottom row cells of the bed)
(to all the bottom row cells of the bed)	

Table 2
Prediction of axial gas velocity and throughflow (U_{th}) velocity at the bubble nose using DEM and TFM

Time (s)	DEM			TFM		
	Axial gas velocity (m/s)	Bubble rise velocity (m/s)	U_{th}/U_{mf}	Axial gas velocity (m/s)	Bubble rise velocity (m/s)	U_{th}/U_{mf}
0.2	9.71	0.68	5.01	10.11	0.68	5.23
0.3	8.20	0.81	4.10	9.82	0.92	4.93
0.4	5.74	0.95	2.66	6.32	1.05	2.92
0.5	4.10	0.48	2.01	5.24	0.56	2.60

istics determined by TFM and DEM approaches. The distinct element method predicts the origin of two small voids above the bubble and below the free surface which is confirmed by the preliminary experimental studies done at Osaka University and TFM fails to predict this property under the similar simulation conditions. There are two characteristic length scales associated in choosing a grid size for TFM, (i) the grid size should be much larger than the individual particle diameter, so that it can accommodate the continuum approximation, and (ii) it should be smaller than the bubble size. In the present case, as a first step, the grid size about 5 particle diameters wide and 5 particles diameter high was chosen to accommodate both the characteristic length scales.

3. Results and discussion

The formation of bubbles is one of the most characteristic phenomena of the gas fluidized beds, many unique properties of the fluidized bed can be directly related to the presence of bubbles and are dominated by their behavior. Therefore, an accurate prediction of parameters such as bubble shape and size, voidage variation, and throughflow velocities are practically important. In this paper, we compare the prediction of all the above parameters determined by DEM with the quantitative predictions from TFM, and qualitatively with the experimental data [5].

In the case of DEM, the predicted characteristics of bubble formation, motion, and eruption at the bed surface are in good qualitative agreement with our preliminary experimental observations [5]. The computed bubble rise velocity, the axial fluid velocity at the bubble nose, and throughflow velocity component are compared with the predictions based on the two fluid model in Table 2. In the present work, $\epsilon > 0.80$ is used for defining the bubble boundary. It is observed that the bubble is detached from the central jet after about $t =$ 0.32 s in both the cases.

The voidage plots as predicted by DEM and TFM are presented in Fig. 3a and b, respectively. The voidage plots predicted by DEM look qualitatively similar to the voidage plots of Halow et al. [24]. In DEM, the increased throughflow from the bubble nose percolates into the bed and produces smaller cavities or bubbles near the bed surface (see Fig. 3a at $t = 0.60$ s). The bubble size is augmented in TFM as it traverses up in Fig. 3b because the gas from the emulsion phase short circuits into the bubble. The key parameter defining particle–particle interactions or in other words the granular stresses, if modeled more accurately, will predict the bubbling characteristics closer to DEM. Actually, TFM does not recognize the discrete nature of the solid's phase, which

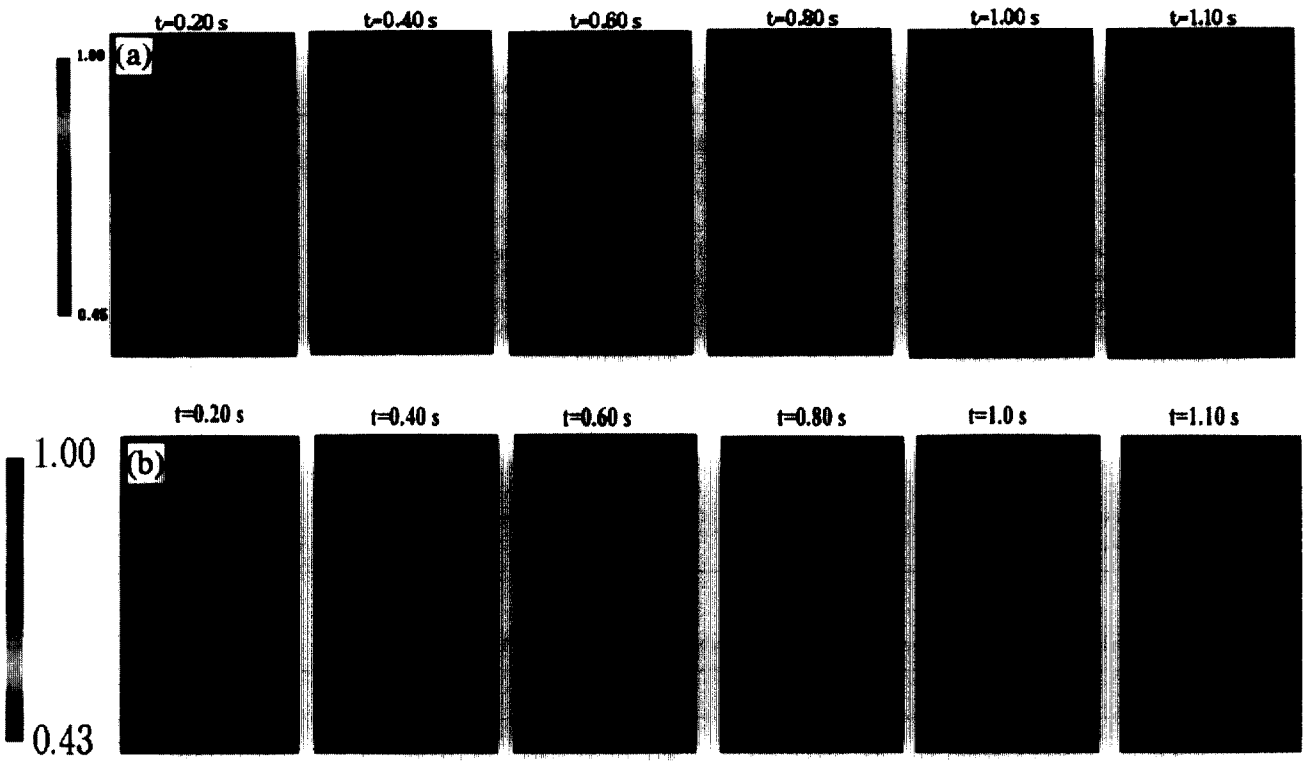

Fig. 3. Voidage plots predicted by (a) Distinct Element Method, (b) Two Fluid Model.

effects the calculation of particle–particle interactions and the drag force. On the other hand, voidage in DEM is calculated by actually counting the number of particles in a particular cell which makes it possible to calculate the particle–particle interactions more precisely. It should be mentioned here that the inter-particle friction plays a critical role in determining the solid's resistance to the fluidizing gas. If the inter-particle friction is neglected or assumed to be negligibly small in TFM then one would expect an unrealistically elongated bubble. If the solid's viscosity is taken to be a very high value then the computations would cease to converge. Typically, in a bubbling bed, particles do not move upward during the bubble formation, but remain at rest until a rising bubble comes to their vicinity. When simulating a fluidizing bed using the Newtonian or power-law model or as an ideal fluid, it is seen that a bubble has a noticeable effect on the particles at a greater distance from the bubble compared to what has actually been observed in the experiments. A Bingham plastic model, which is like a rigid material that ceases to flow until an applied shear stress exceeds the yield stress, would ascertain that the particles are at rest until the rising bubble comes to their vicinity. In such a model, due to the lack of the available experimental data on solid's viscosity of different powders, one will have to heuristically determine the yield stresses. It is anticipated that such a model if applied to the fluidizing bed would yield bubble shapes and bubbling characteristics much similar to DEM simulations and experiments.

In case of no damping in DEM, that is, when the coefficient of restitution $e = 1$, the particles would not dissipate any energy in the collisions. In such a configuration, particles above the bubble roof (where there is a maximum drag experienced by the particles) would move with the higher velocities as compared to the case with the viscous damping—which would give rise to distorted bubble shapes and many small cavities or voids in the vicinity of the bubble roof.

The particle mixing, based on the collision dynamics of individual particles, is presented in Fig. 4a. Some of the salient features of the DEM are its prediction of raining of particles inside the bubble, and more realistic mixing patterns. The raining of particles (see Fig. 4a, at $t = 0.80$ s) from the bubble roof could be explained by the comparing the magnitudes of drag force and the weight of the particles. At the bottom region of the bubble roof where the porosity is high and the drag force is not sufficient enough to sustain the weight of the particles, causes the particles to fall from the bubble roof.

Since, the individual particle motion cannot be determined in TFM, we predict the deformation of colored particle layers based on the locally averaged particulate velocities in a grid cell. To give a one-to-one comparison, deformation of the particle layers in DEM is also calculated by averaging the velocities of the individual particles in a grid cell. Particulate mixing in TFM is calculated by assigning the particulate phase velocity of a particular grid cell to the center of the ball. Essentially, in this formulation, all the rectangular grid cells of 2×2 cm are replaced by the balls of diameter 2 cm.

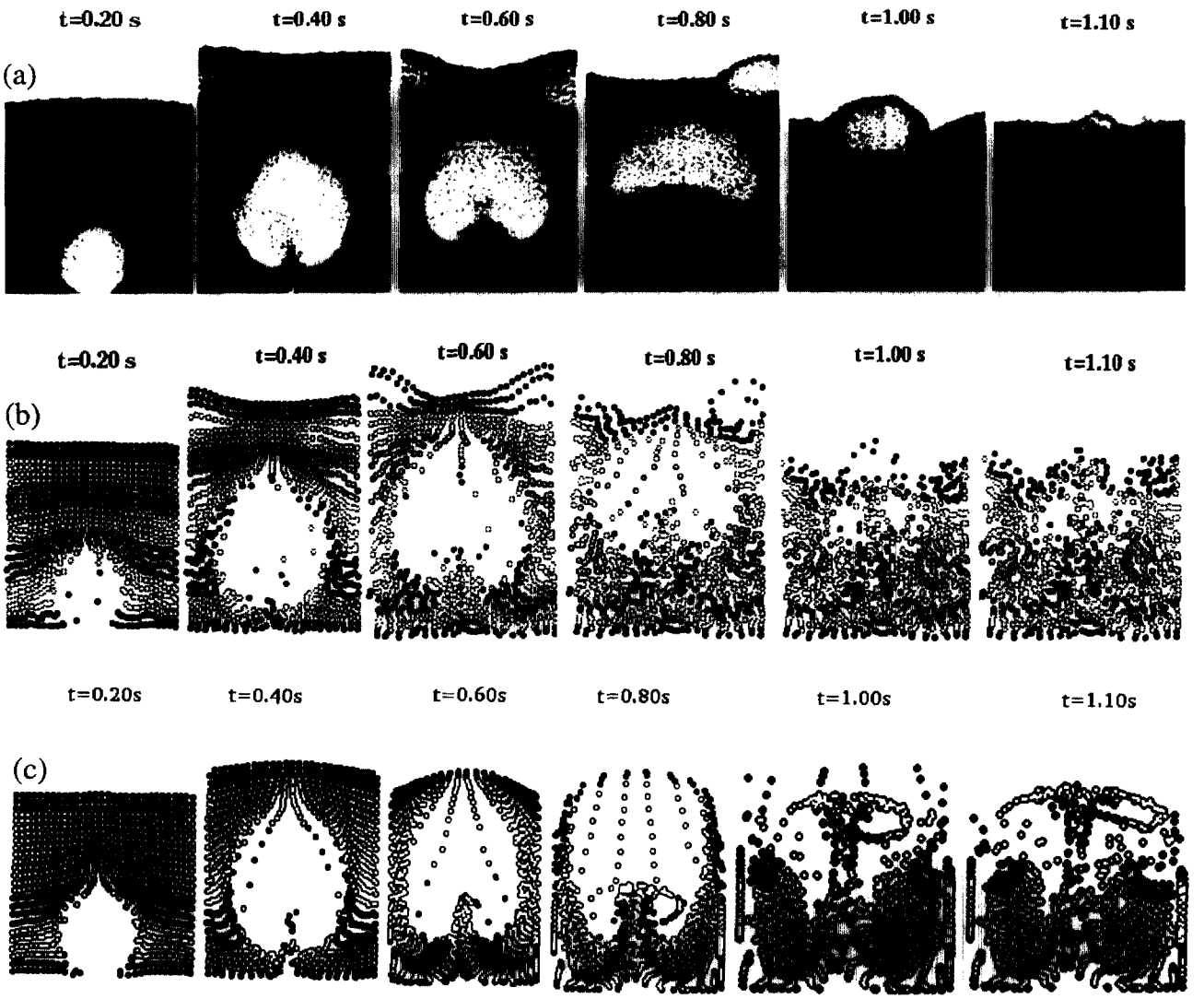

Fig. 4. Deformation of particles layers based on (a) individual particle velocities in DEM, (b) averaged particle velocities of a grid cell in DEM, and (c) averaged particle velocities of a grid cell in TFM.

At time $t=0$ s, all the balls are considered to be at rest and assigned a particular color to observe the mixing patterns during the fluidization process. At time $t=\Delta t$, each ball moves a distance of $v_{sx}\Delta t$ in the horizontal direction and $v_{sy}\Delta t$ (where v_{sx} and v_{sy} are the particulate velocities in the horizontal and vertical direction in that particular grid cell) in the vertical direction. In the next time step, i.e., $t=2\Delta t$, the balls will acquire the new grid velocities of the cell (calculated by TFM in the next time step) in which they are located, and it should be noted that no collision dynamics is applied in calculating the positions of the balls. That is why, some balls overlap on the other balls and give a feeling as if the channeling of flow has occurred during the fluidization process. Visual glance at the Fig. 4b and c gives an impression that if there is a channeling of flow occurring after $t=0.80$ s in TFM and after $t=1.0$ s in DEM; the reason for such big cavities in these figures is that some of the balls are overlapping on other balls, and there is no collision dynamics used in the prediction of the position of the balls.

It is evident from Table 2 that the axial fluid velocity at the nose of the bubble in TFM is higher than the velocity predicted by DEM, which essentially indicates that there is a less resistance being offered by the solid's phase. It is observed that gas percolation from the bubble nose to the emulsion in TFM is less than for DEM simulations.

The summary of the salient features along with the advantages and disadvantages of DEM and TFM are given in Table 3. It could be seen from the foregoing analysis that the particle–particle interaction which is included in TFM through solid's pressure, P_s, is a sensitive key parameter, and needs to be tuned-in for each case running with the different physical properties. Inaccurate determination of the empirical correlations for solid's pressure (either through the experiments or the kinetic theory of granular media) would hinder the true bubbling characteristics of the fluidized beds in TFM. However, in DEM the variation in the empirical input of spring stiffness or frictional coefficient would not alter the bubble characteristics significantly.

Table 3
Summary of the salient features of discrete element method and two fluid model

S. No.	Distinct Element Method (DEM)	Two Fluid Model (TFM)
1.	It is possible to account for the individual particles' shape, size, and density. For example, a particle shape approximated by an 'n-sided' polygon can be incorporated in this model.	Particles are characterized by their mean size and density. Different sizes and densities of the particles are treated as the separate phases which would increase the number of conservation equations to solve.
2.	Individual particle motion can be traced.	Only averaged particulate motion in a grid cell can be computed.
3.	Particle interactions are calculated from coefficient of restitution (e) and friction (μ) between the particles. Different values of (e) can be given for particle–particle collisions and particle–wall collisions.	Particle interaction is normally expressed as a function of porosity and is calculated empirically. Using kinetic theory of granular media, it may also be calculated by the empirical input of coefficients of restitution (e) and friction (μ).
4.	Computational time depends on the calculation of particle motion explicitly, and three (1 continuity and 2 momentum equations for a 2-D case) sets of equations for fluid motion iteratively. A typical 1 second simulation on a real time scale with 22 000 particles and a time step of 2.0×10^{-4} s takes roughly 6 h on Hewlett Packard workstation. It should be mentioned that CPU time depends on the tolerance criterion used for the convergence given by two methods. Scaling-up or similitude analyses need to be performed to make it an attractive commercial choice.	Computational time depends on the iterative solutions of six sets of simultaneous differential equations. A typical calculation of 15×50 cells takes about 4 h on a Silicon Graphics work station. For large number of particles, for example in millions, the CPU time would be comparatively very small then the CPU time required by DEM.
5.	Stability of calculations forces the time step to be sufficiently smaller than $2\pi(m/k)^{1/2}$ where k is the spring constant, m is the mass of an individual particle. Integration time step is normally increased by artificially decreasing the stiffness of the interactions.	The time step should be less than $\Delta y/V_{max}$, where Δy is the vertical grid spacing, and V_{max} is the maximum fluid velocity.
6.	It can predict the raining of individual particles into the bubble from its roof.	Prediction of raining of individual particles is not possible, however, the average voidage inside the bubble is decreased probably due to entry of particles from its wake.
7.	Considers multiple collision of particles, based on the soft sphere approach of the molecular dynamics. Hard sphere approach, based on binary instantaneous collisions is also used in the literature.	No such considerations.
8.	It is possible to allow the particles to fall under the gravity to simulate fixed bed conditions. Voidage at minimum fluidization is calculated from the number of individual particles in a grid cell.	Voidage as an initial condition of the fluidization needs to be specified. Compaction gas phase volume fraction (ϵ^*) needs to be specified. Particle–particle interaction, which is empirically modeled through the solids elasticity, is a very strong function of ϵ^*.
9.	Visualization of the individual particle mixing is possible.	Mixing characterized by integrating the averaged particulate phase velocity to obtain the estimated position of the particles is possible. Particulate mixing is driven by the convection and diffusion processes. Particulate diffusion must be modeled empirically.
10.	Minimum grid size tried for this method was 1×1 cm. If grid size chosen smaller than this value would affect the accuracy of the voidage computations.	To accommodate the 'continuum' or averaging approximation, and for the convergence, a first successful convergent solution was obtained with the grid height and width of at least five particles diameters. This is the reason for choosing a coarse grid size of 2×2 cm.

4. Conclusions

The predicted characteristics of the bubble formation, motion, and eruption at the bed surface from Distinct Element Method are compared with the Two Fluid Model. It is inferred that the inter-particle friction which is incorporated in TFM through the solid's pressure and viscosity are the very sensitive key parameters, and needs to be tuned-in for each case running with the different set of physical properties. Inaccurate determination of the empirical correlations for solid's pressure either through the experiments or through the kinetic theory of granular media would hinder the true bubbling characteristics of the fluidized beds in TFM. It is anticipated that the Bingham plastic model for the solid's rheology would predict the more realistic bubble shapes. DEM does not require any empirical input of solid's rheology which makes it more appropriate for some modeling situations. For the simulations of small beds, the computational time required by TFM and DEM are comparable, but if one requires to model a system with the millions of particles then TFM would take very small time as compared to the DEM.

Acknowledgements

This material is based upon work supported by the National Science Foundation under Grant no. INT-9424422. Any opinions, findings, and conclusions or recommendations expressed in this material are those of the authors and do not necessarily reflect the views of the National Science Foundation. One of the authors (DG) would like to thank Dr. Madhava Syamlal and Dr. T.J. O'Brien of METC for their valuable comments during the preparation of this manuscript.

References

[1] J.F. Davidson, Symposium on fluidization—discussion, Trans. Inst. Chem. Eng. 39 (1961) 230–232.
[2] R. Jackson, The mechanics of fluidized beds: Part I, Trans. Inst. Chem. Eng. 41 (1963) 13–20.
[3] T.B. Anderson, R. Jackson, A fluid mechanical description of fluidized beds, I&EC Fundam. 6 (4) (1967) 527–539.
[4] Y. Tsuji, T. Tanaka, T. Ishida, Lagrangian numerical simulation of plug flow of cohesion less particles in a horizontal pipe, Powder Technol. 71 (1992) 239–250.
[5] Y. Tsuji, T. Kawaguchi, T. Tanaka, Discrete particle simulation of two-dimensional fluidized bed, Powder Technol. 77 (1993) 79–87.
[6] B.P.B. Hoomans, J.A.M. Kuipers, W.J. Briels, W.P.M. Van Swaiij, Discrete particle simulation of bubble and slug formation in a two-dimensional gas-fluidized bed: a hard sphere approach, Chem. Eng. Sci. 51 (1996) 99–118.
[7] M. Syamlal, W. Rogers, T.J. O'Brien, MFIX Documentation: Theory Guide, Technical Note, DOE/METC-94/1004, NTIS/DE 94000087, Springfield, VA, 1993.
[8] P.A. Cundall, O.D.L. Strack, Discrete numerical model for granular assemblies, Geotechnique 29 (1979) 47–65.
[9] J.D. Gabor, On the mechanics of fluidized particle movement, Chem. Eng. J. 4 (1972) 118–126.
[10] D. Gidaspow, Multi phase Flow and Fluidization: Continuum and Kinetic Theory Description, Academic Press, New York, 1994.
[11] C.K.K. Lun, S.B. Savage, D.J. Jeffrey, N. Nichepurniy, Kinetic theories for granular flow: inelastic particles in couette flow of singly inelastic particles in a general flow field, J. Fluid Mechanics 140 (1984) 223–256.
[12] S.M.P. Musters, K. Rietema, The effect of interparticle forces on the expansion of a homogeneous gas-fluidized bed, Powder Technol. 18 (1977) 239–248.
[13] R.R. Cranfield, D. Geldart, Large particle fluidization, Chem. Eng. Sci. 29 (1974) 935–947.
[14] J.G. Yates, D.J. Cheesman, Y.A. Sergeev, Experimental observations of voidage distribution around bubbles in a fluidized bed, Chem. Eng. Sci. 49 (12) (1994) 1885–1894.
[15] D. Gidaspow, Y.C. Seo, B. Ettehadieh, Hydrodynamics of fluidization: experimental and theoretical bubble sizes in a two-dimensional bed with a jet, Chem. Eng. Commun. 22 (1983) 253–272.
[16] L.R. Glicksman, M.R. Hyre, P.A. Farrell, Dynamic similarity in fluidization, Int. J. Multi phase Flow 20 (1994) 331–386.
[17] M. Syamlal, T.J. O'Brien, Computer simulation of bubbles in a fluidized beds, AIChE Symp. Ser. 85 (270) (1989) 22–31.
[18] M. Syamlal, T.J. O'Brien, Simulation of granular layer inversion in liquid fluidized beds, Int. J. Multi phase Flow 14 (1988) 473–481.
[19] M. Massoudi, K.R. Rajagopal, J.M. Ekmann, M.P. Mathur, Remarks on the modeling of fluidized systems, AIChE J. 38 (1992) 471–472.
[20] J.A.M. Kuipers, K.J. Van Duin, F.P.H. Van Beckum, W.P.M. Van Swaiij, Numerical model of gas-fluidized beds, Chem. Eng. Sci. 47 (1992) 1913–1924.
[21] D. Gidaspow, Hydrodynamics of fluidization and heat transfer: supercomputer modeling, Appl. Mechanics Rev. 39 (1986) 1–23.
[22] A. Sokolichin, G. Eigenberger, A. Lapin, A. Lubbert, Dynamic numerical solution of gas–liquid two phase flows Euler/Euler vs. Euler/Lagrange, Chem. Eng. Sci. 52 (1997) 611–626.
[23] D. Gera, M. Gautam, D.W. Lyons, Y. Tsuji, Numerical Simulation of Large Particles Fluidized Bed: TFM vs. DEM Approach, Fludization-IX, Durango, CO, May 17–22, 1998.
[24] J.S. Halow, G.E. Fasching, P. Nicoletti, J.L. Spenik, Observations of a fluidized bed using capacitance imaging, Chem. Eng. Sci. 48 (1993) 643–659.